Virology 536 (2019) 58–67

Contents lists available at ScienceDirect

Virology

journal homepage: www.elsevier.com/locate/virology

The evolution and characterization of influenza A(H7N9) virus under the selective pressure of peramivir

Yiyue Ge[a,*,1], Ying Chi[a,1], Xiaoyan Min[b,1], Kangchen Zhao[a], Bin Wu[a], Tao Wu[a], Xiaojuan Zhu[a], Zhiyang Shi[a], Fengcai Zhu[a], Lunbiao Cui[a,**]

[a] Institute of Pathogenic Microbiology, NHC Key Laboratories of Enteric Pathogenic Microbiology, Jiangsu Provincial Center for Disease Control and Prevention, Nanjing, 210009, China
[b] Department of Geriatric Cardiology, The First Affiliated Hospital of Nanjing Medical University, Nanjing, 210029, China

ARTICLE INFO

Keywords:
H7N9
Influenza virus
Quasispecies
Evolution
Selective pressure
Neuraminidase
Peramivir
Mutation

ABSTRACT

Human infection with H7N9 virus has provoked global public health concern due to the substantial morbidity and mortality. Neuraminidase inhibitors (NAIs) are used as first-line drugs to treat the infection. However, virus quasispecies can evolve rapidly under drug pressure, which may alter various biological characteristics of virus. Using an *in vitro* evolution platform and next-generation sequencing, we found the presence of peramivir led to changes to the dominant populations of the virus. Two important amino acid substitutions were identified in NA, I222T and H274Y, which caused reduced susceptibilities to oseltamivir or both oseltamivir and peramivir as confirmed by enzyme- and cell-based assays. The NA-H274Y variant showed decreased replicative fitness at the early stage of infection accompanied with impaired NA function. The quasispecies evolution of H7N9 virus and the potential emergence of these two variants should be closely monitored, which may guide the adjustment of antiviral strategies.

1. Introduction

Influenza A virus (IAV) causes both annual epidemics and occasional pandemics, which remains a major public health concern throughout the world (Taubenberger and Kash, 2010). Since its first emergence in March 2013 in China, avian-origin influenza A(H7N9) virus has caused five waves of human infections, including 1567 cases and at least 615 deaths (Gao et al., 2013; WHO, 2018). Also, numbers of imported H7N9 cases have been found in other countries, indicating sustained transmission of the virus (Iuliano et al., 2017; Lu et al., 2018; WHO, 2018). By using the Influenza Risk Assessment Tool (IRAT), influenza A(H7N9) virus has been reported to present the highest risk among all evaluated novel influenza viruses in terms of potential to emerge as a pandemic virus and cause substantial human illness (CDC, 2017).

Due to error-prone replication by RNA-dependent RNA polymerases, RNA viruses have high levels of mutation and exist as quasispecies (genetically diverse populations) (Drake and Holland, 1999). Quasispecies evolution is influenced by high mutation rates and the existence of selective pressures, such as environment, host and drug pressure (Domingo et al., 2012). To overcome internal or external selective constraints, the fittest variants in quasispecies will be gradually screened out and become the dominant gene cluster. Just as many other RNA viruses, H7N9 virus also existed as quasispecies (Xiao et al., 2018). The evolution of quasispecies characterized by mutation accumulation is a great opportunity for H7N9 viruses to change their biological characteristics such as antigenicity, drug resistance and pathogenicity in order to escape from neutralizing antibody, antiviral drugs as well as cytotoxic T-cell (Lu et al., 2018; Marjuki et al., 2015). Previous studies suggested that the H7N9 virus had evolved into two distinct genetic lineages, the Pearl River Delta lineage and the Yangtze River Delta lineage (Wang et al., 2016). In contrast to Pearl River Delta lineage, virus in Yangtze River Delta lineage appears to exhibit reduced antigenic relatedness with the existing candidate H7N9 vaccine virus stocks (Iuliano et al., 2017; Zhu et al., 2017). Data showed that most recent human infections were caused by virus belonging to the Yangtze River Delta lineage, a subset of which had acquired a highly pathogenic phenotype (Yu et al., 2019). Thus, a detailed understanding of H7N9 virus quasispecies evolution is of great importance and imperative.

Sequence analysis of the H7N9 genome revealed the presence of

* Corresponding author.
** Corresponding author.
E-mail addresses: geyiyue@163.com (Y. Ge), lbcui@jscdc.cn (L. Cui).
[1] These authors contributed equally to this work.

https://doi.org/10.1016/j.virol.2019.08.004
Received 6 May 2019; Received in revised form 5 August 2019; Accepted 5 August 2019
Available online 06 August 2019
0042-6822/

S31 N substitution in the M2 protein, indicating resistance to amantadine (Gao et al., 2013). Oseltamivir, zanamivir and peramivir are currently approved neuraminidase (NA) inhibitor (NAI) for H7N9 treatment in China. However, a great challenge in the treatment of H7N9 virus with NAI is the emergence of drug-resistant mutants under the selective pressure (Hu et al., 2013). Since H7N9 outbreak in 2013, several resistant sites of the virus have been reported, such as R292K, E119V and H274Y (Marjuki et al., 2015; Wang et al., 2016; Yang et al., 2017). Mutations in the NA active sites not only lead to drug resistance, but also can affect enzymatic activity, virus fitness and pathogenicity (Marjuki et al., 2015; Zhang et al., 2014). Therefore, comprehensive analysis of quasispecies evolution and mutagenesis of H7N9 virus under drug pressure is very important for disease prevention and treatment.

However, most of the reported drug-resistant mutations of H7N9 virus were found in sporadic cases but not in systematic study. Also, how the development of resistance affects H7N9 virus quasispecies remains unclear. In the present study, by using an *in vitro* evolution platform and next-generation sequencing (NGS) technology, we systematically traced the evolutionary trajectories of H7N9 virus quasispecies under the selective pressure of peramivir, and then analyzed the effects of key amino acid substitutions in NA caused by quasispecies evolution on the biological characteristics of the virus. We found that H7N9 virus quasispecies evolved under the antiviral pressure of peramivir, leading to changes to the dominant populations of the virus. Moreover, we identified two important amino acid substitutions in NA, I222T and H274Y (N2 system numbering), between which I222T was first identified in 2013 H7N9 virus. Finally, the drug resistance profile, fitness and enzymatic activity of the variants were investigated. Our results indicate that the quasispecies evolution of H7N9 virus and the potential emergence of NA-I222T and NA-H274Y variants should be closely monitored, which may guide the adjustment of antiviral strategies.

2. Materials and methods

2.1. Cells, virus, and compounds

Madin-Darby canine kidney (MDCK) cells were obtained from the American Type Culture Collection (ATCC). A/Nanjing/2/2013(H7N9) virus strain isolated from a patient specimen at Jiangsu Provincial Center for Disease Control and Prevention (CDC) was propagated 3 passages in MDCK cells to establish a viral stock (termed as Passage 1) for serial passage. Four NAIs (oseltamivir, peramivir, zanamivir and Laninamivir) and two non-NAIs (favipiravir (T705) and ribavirin) were included in this study. Oseltamivir carboxylate, peramivir trihydrate, zanamivir, T705 and ribavirin were purchased from MedChemexpress CO., Ltd, (Monmouth Junction, NJ, USA). Laninamivir was purchased from TRC (Toronto, Ontario, Canada). These compounds were dissolved in deionized water at initial concentrations of 0.5 mM - 10 mM. All infectious experiments were carried out in the biosafety level 3 (BSL3) laboratory at Jiangsu Provincial CDC.

2.2. Determination of viral titer

The infectious titers of H7N9 viruses were determined in MDCK cells by 50% tissue culture infectious dose ($TCID_{50}$) assay as described by World Health Organization (WHO) (WHO, 2013). Briefly, a half log_{10} dilution series was performed on the virus samples with dulbecco's modified eagle medium (DMEM, ThermoFisher Scientific, MA, USA) containing 1% bovine serum albumin (BSA, Sigma-Aldrich, MO, USA), 1% penn/strep (Gibco, Grand Island, NY, USA) and 2 μg/ml tosyl phenylalanyl chloromethyl ketone (TPCK)-trypsin (Sigma-Aldrich, MO, USA) in 96-well plates. Then 1.5×10^4 MDCK cells were added to each well. After incubation at 37 °C in 5% CO_2 for 20 h, cells were washed with phosphate-buffered saline (PBS) and fixed with cold 80% acetone. Finally, the presence of influenza A nucleoprotein (NP) protein in infected cells was detected by enzyme-linked immunosorbent assay (ELISA) and the $TCID_{50}$ was calculated by the Reed-Muench method.

2.3. Serial passage of H7N9 virus under the selective pressure of peramivir

Confluent MDCK cells in 12-well plates were inoculated with H7N9 viral stock (Passage 1) diluted in influenza virus growth medium (DMEM supplemented with 0.5% BSA, 1% penn/strep and 2 μg/ml TPCK-trypsin) supplemented with appropriate concentration of peramivir in triplicates. After adsorption for 1 h at 37 °C, cells were washed once with PBS, added with 1 ml of the same medium, and incubated at 37 °C for several days until the culture reached > 90% cytopathic effect (CPE). Cell-free supernatants were collected, and the virus titers were determined by real-time RT-PCR assay (Li et al., 2013) and $TCID_{50}$ assay. The supernatants were then used to infect a new cell monolayer (the next passage), or kept at -80 °C until further use. The multiplicity of infection (MOI) was 0.01 $TICD_{50}$ per cell for the initial infection, and was later determined to be 0.001 to 0.1 $TICD_{50}$ per cell for additional passages. The concentration of peramivir in the first round of selection was 1 × the 50% inhibitory concentration (IC_{50}) for Passage 1 virus as determined by probit regression, and it was doubled in each subsequent passage. If > 90% CPE couldn't be generated, the concentration of peramivir was escalated at a lower rate. In the removal test of drug pressure, peramivir was deliberately withdrawn.

2.4. Enzyme-based NA inhibition assay and NA kinetics

The susceptibilities of H7N9 viruses to different NAIs were determined with enzyme-based NA inhibition assays by using the NA-XTD™ Influenza Neuraminidase Assay Kit (ThermoFisher Scientific, MA, USA) according to the manufacturer's instructions. After the measurement of chemiluminescent signal using a SpectraMax M5 Multi-Mode Microplate Reader (Molecular Devices, Sunnyvale, CA, USA), the IC_{50} values were estimated by variable-slope dose-response curve fitting using GraphPad Prism software. The NA enzymatic kinetics were measured as previously described using the 2′-(4-methylumbelliferyl)-α-D-*N*-acetylneuraminic acid (MUNANA) substrate (final concentration, 0–1600 μM) (Yen et al., 2013). The fluorescence was monitored every 60 s for 60 min using the SpectraMax M5 Multi-Mode Microplate Reader (Molecular Devices) with excitation and emission wavelengths of 335 and 460 nm, respectively. The Michaelis constant (K_m) and maximum velocity (V_{max}) values of substrate conversion were determined by fitting enzyme kinetic data to the Michaelis-Menten equation using GraphPad Prism.

2.5. Viral RNA isolation and NGS

Viral RNA was isolated with a QIAamp Viral RNA Mini Kit (Qiagen, Valencia, CA, USA) according to the manufacturer's instructions. The first-strand cDNA was synthesized by using TaKaRa Primescript Reverse Transcriptase (TaKaRa Biotechnology Co. Ltd., Dalian, People's Republic of China) and a Uni12 primer (5′-AGCRAAAGCAGG-3′). The RT reaction was performed at 50 °C for 60 min. After the degradation of RNA strands from RNA/DNA hybrids by adding Ribonuclease H (RNase H), seven universal reverse primers (PB2、PB1、PA、HA、NP、M and NS) for all influenza A viruses and a N9-specific reverse primer (N9) (Supplemental Table S1) (Hoffmann et al., 2001), as well as 2.5 U of Klenow fragment polymerase (NEB, Ipswich, USA) were used for the second-strand synthesis which was performed at 37 °C for 1 h. Then the double-strand cDNA was purified and used to construct a DNA library with a Nextera XT Library Preparation Kit (Illumina, San Diego, CA, USA) according to the manufacturer's instructions. Briefly, samples were first fragmented and tagged with adapters, then amplified by a limited-cycle PCR to add the barcodes, and finally purified and size-selected by using AMPure XP Beads (Beckman coulter, Brea, CA, USA). The quality of the libraries was checked on High Sensitivity DNA Chips

on a Bioanalyzer 2100 (Agilent Technologies, Palo Alto, CA, USA). Equimolar amounts of normalized libraries were combined before the paired-end read (2 × 150 bp) sequencing run was performed on a MiSeq system (Illumina).

2.6. Analysis of sequencing data

The sequencing reads with the same barcode were assigned to a sample to generate FASTQ files on the instrument. These files were imported into the CLC Genomic Workbench 7.5.1 (CLC Bio, Qiagen) for further analysis. First, the imported reads were trimmed to a quality score limit of 0.001 (Q30) with maximum 2 ambiguous nucleotides. The reads with length below 50 nucleotides were also removed. Next, the trimmed reads were mapped to the reference genome of A/Nanjing/2/2013(H7N9) virus (GISAID, accessions EPI497811-EPI497812, EPI497814-EPI497818 and EPI497826). Finally, the quality-based variant detection was performed for calling of single-nucleotide variants (SNVs) with settings the neighborhood radius of 5, the maximum gap and mismatch count of 2, the minimum central quality of 20, the minimum coverage of 20, and the minimum variant frequency of 5%. If the variant frequency was ≥95%, the variant was considered homogeneous and vice versa heterogeneous.

2.7. Plaque purification of variants

Briefly, confluent monolayers of MDCK cells in 12-well plates were inoculated with six 10-fold serial dilutions of H7N9 viruses in triplicates, then incubated for 1 h at 37 °C (rocked every 20 min), and washed with PBS. Equal volumes of 1.6% low melting point (LMP) agarose kept at 56 °C and 2 × minimum essential medium (MEM) (1% BSA, 2% penn/strep, 4 μg/ml TPCK-trypsin and 32 μM peramivir) kept at 37 °C were mixed, and 1 ml of the mixture was added to each well. Then the plates were incubated at 37 °C in 5% CO_2 for 48–72 h. When plaques were visible, each well was overlaid with 200 μl of 3-(4, 5-dimethyl-2-thiazolyl)-2, 5-diphenyl-2H-tetrazolium bromide (MTT, 5 mg/ml, Sigma-Aldrich) and further incubated for 2–3 h. Finally, plaques were picked and used to infect new confluent monolayers of MDCK cells. The whole genome sequences of purified variants were analyzed by NGS.

2.8. Virus yield reduction assay

To evaluate the sensitivities of plaque-purified variants to NAIs and non-NAIs at the cellular level, confluent MDCK cells in 96-well plates were inoculated with H7N9 viruses at a MOI of 0.005 $TICD_{50}$ per cell and cultured in the absence or presence of various concentrations of antiviral compounds (oseltamivir carboxylate and peramivir: 0.013 μM - 1000 μM, ribavirin and T705: 0.0064 μM - 100 μM) in triplicates. At 24 h post infection, cell-free supernatants were collected. Viral RNA was isolated from 140 μl of each specimen, and the relative expression levels of H7 gene at different drug concentrations were quantified by real-time RT-PCR and normalized to control (no drug). The IC_{50} value of each drug was determined by variable-slope dose-response curve fitting using GraphPad Prism software.

2.9. Viral replication kinetics

Confluent monolayers of MDCK cells in 48-well plates were inoculated with plaque-purified variants and their controls at a MOI of 0.005 $TICD_{50}$ per cell and incubated at 37 °C in 5% CO_2. Cell-free supernatants were collected at 12, 24, 36, 48, 60 and 72 h post infection. The viral titers were determined by $TCID_{50}$ assay as described before.

2.10. Statistical analysis

Data was presented as mean ± standard deviation (SD). Statistical analyses were performed using SPSS software version 19.0 (IBM SPSS, Inc., Chicago, USA). One-way analysis of variance (ANOVA) with post hoc analysis using least significant difference (LSD) test was performed to compare the viral titers among different groups. $P < 0.05$ was considered statistically significant.

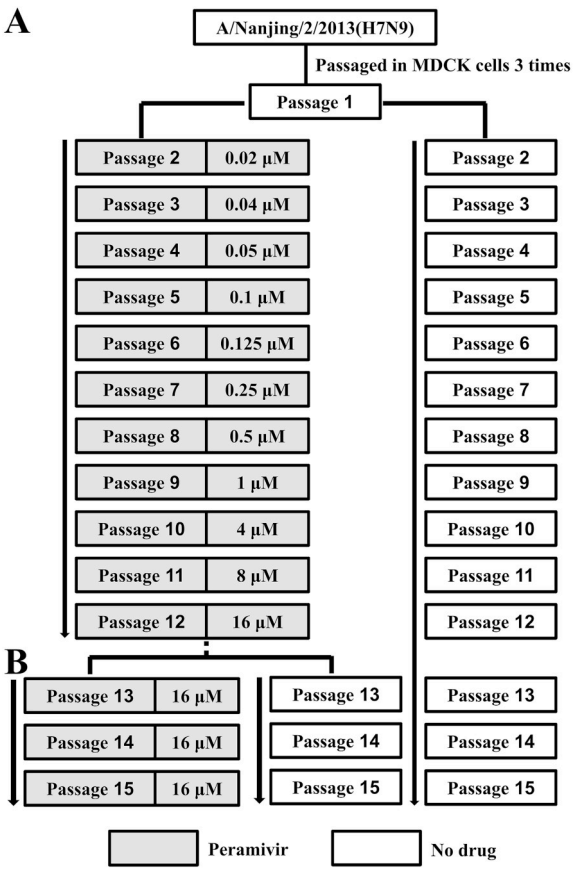

Fig. 1. Experimental schemes. (A) A/Nanjing/2/2013(H7N9) virus was passaged 3 times in MDCK cells to establish a viral stock (termed as Passage 1) for serial passage with or without the selective pressure of peramivir. (B) In the removal test of drug pressure, peramivir was deliberately withdrawn from passage 13 to passage 15. All experiments were performed in triplicate (in parallel) from passage 2.

3. Results

3.1. Obtainment of different generations of H7N9 viruses selected by drug pressure

Experimental schemes for serial passage of H7N9 viruses in MDCK cells with or without the selective pressure of peramivir, as well as drug withdrawal beyond passage 12 are summarized in Fig. 1. The IC_{50} value of peramivir for Passage 1 virus was determined to be 0.02 μM which was used as the initial concentration for selection. The actual concentration of peramivir used in each round of selection is showed in Fig. 1A. By passage 6, the susceptibilities of the virus pools to oseltamivir carboxylate and peramivir were examined by enzyme-based NA inhibition assay. As shown in Supplemental Table S2, No significant difference was found between the virus pools of the experimental group and Passage 1 virus. However, by passage 12, two parallel wells of virus from triplicates treated with peramivir, Passage 12-P2 and Passage 12-P3, exhibited significantly decreased susceptibilities (7.54-fold and 88.89-fold, respectively) to oseltamivir carboxylate as compared with control. The susceptibility of Passage 12-P3 to peramivir was also decreased (8.10-fold). All the virus pools from passage 1 to 12 were collected for virus quasispecies analysis.

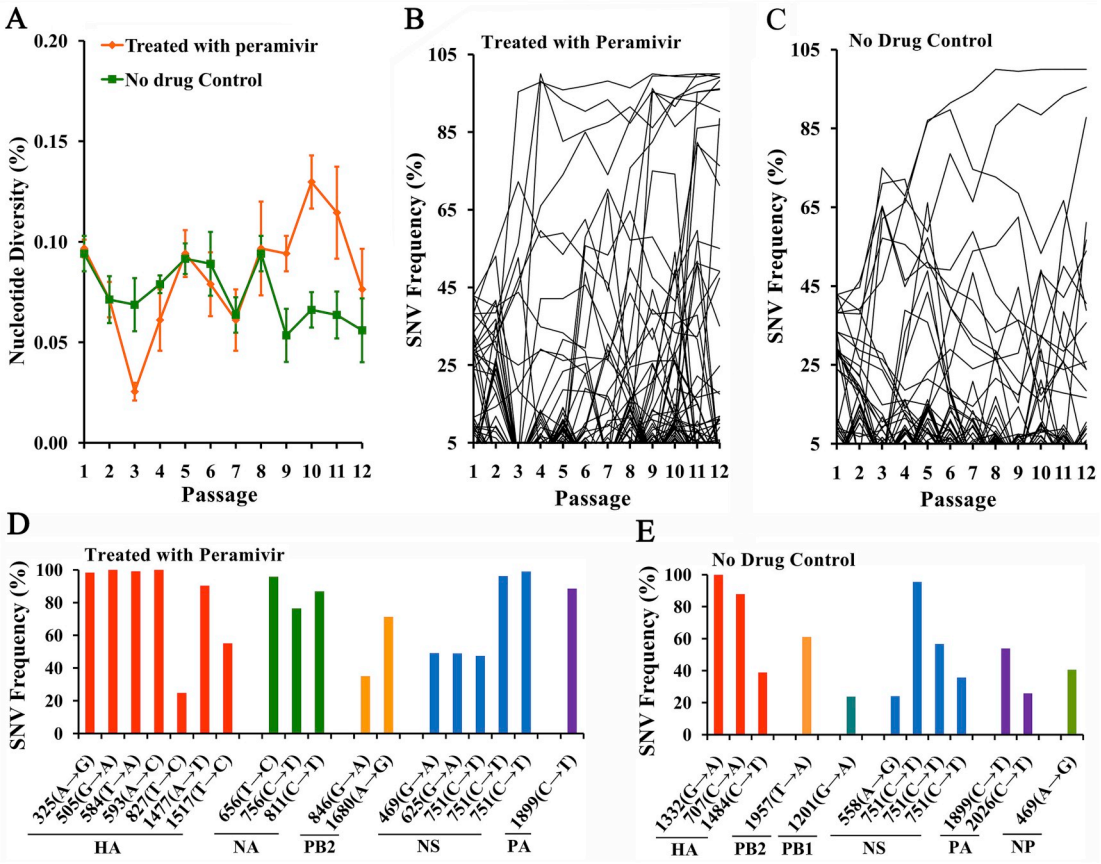

Fig. 2. The changes of population diversity and SNP frequency during serial passage in the presence and absence of peramivir. (A) The genomewide nucleotide diversity of H7N9 virus was measured for each passage of growth. Data are expressed as mean ± SD from triplicates. (B and C) The frequencies of all SNVs across viral genome were tracked for 12 passages with (B) or without (C) the selective pressure of peramivir. The data for both groups are based on the results from triplicates. Each data line represents the frequencies of one SNV from a replicate tracked for 12 passages. (D and E) All the SNVs with mutation frequencies over 20% at passage 12 in peramivir-treated group (D) and control group (E) are showed. The abscissa indicates the mutation positions and the base changes for the SNVs from each replicate.

Table 1
The emerged SNVs and the corresponding changes of amino acids in NA under the selective pressure of peramivir.

Passage	Sample[b]	Position	Reference	Variant	Frequency (%)	Amino acid change Ref→(Residue)[a]→Var
4	P1	1321	G	A	6.58	I444V
5	P1	1321	G	A	5.32	I444V
6	P1	1321	G	A	9.26	I444V
	P3	1338	T	C	9.09	None
7	P3	1338	T	C	30.43	None
8	P3	791	C	G	5.00	S267C
		1338	T	C	17.14	None
9	P1	1321	G	A	7.02	I444V
10	P2	656	T	C	9.68	I222T
		756	C	T	10.53	None
	P3	811	C	T	39.82	H274Y
		1338	T	C	7.78	None
11	P1	503	G	A	7.94	S171 N
		1321	G	A	10.63	I444V
	P2	656	T	C	95.31	I222T
		756	C	T	81.67	None
	P3	811	C	T	86.00	H274Y
		1033	G	A	5.56	V349I
12	P2	656	T	C	95.89	I222T
		756	C	T	76.36	None
	P3	811	C	T	86.90	H274Y
		1033	G	A	10.79	V349I

[a] N2 system numbering.
[b] P1, P2 and P3 refer to triplicate parallel wells of virus treated with peramivir.

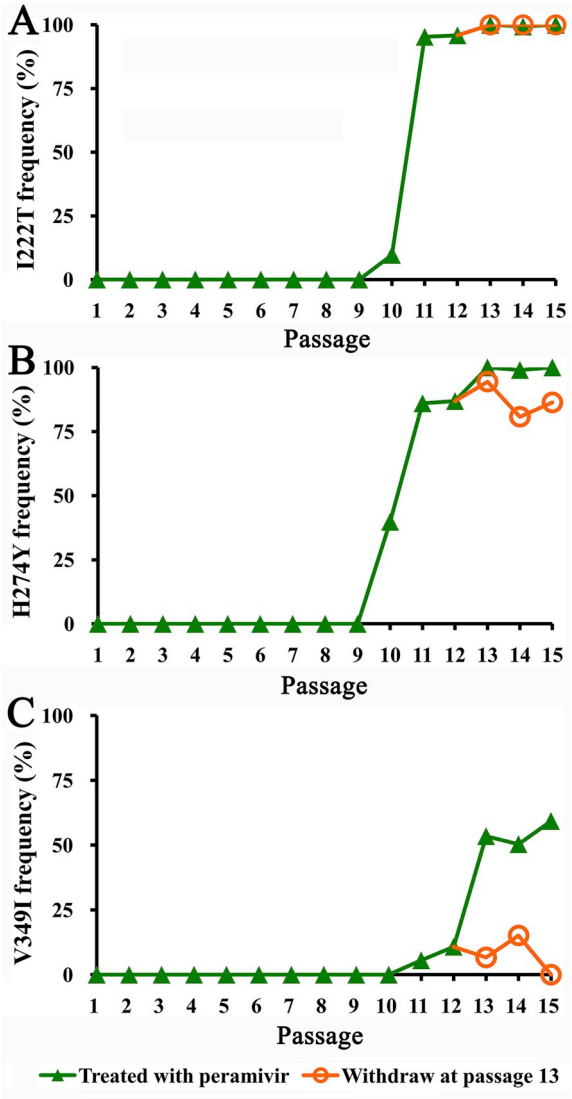

Fig. 3. Effect of peramivir withdrawal on the frequencies of I222T, H274Y and V349I quasispecies. After passage 13, peramivir was either continued or withdrawn for 3 additional passages. The frequencies of I222T (A), H274Y (B) and V349I (C) in experimental and control groups were detected by high-throughput sequencing.

Table 2
Comparison of amino acid sequences of plaque-purified variants and Passage 1 virus.

Virus	NA[a]				HA[b]		
	222	274	101	160	186	189	483
Passage 1	I	H	K	A/T[c]	V	E/A[c]	N
NA-I222T	**T**	H	K	A	**E**	E	N
NA-H274Y	I	**Y**	**E**	T	V	A	**Y**

[a] N2 system numbering.
[b] H3 system numbering.
[c] If the frequency of amino acid substitution was lower than or equal to 95%, the existence of quasispecies was considered.

3.2. The quasispecies polymorphism and evolution of H7N9 virus under the selective pressure of peramivir

To investigate the dynamic change of virus quasispecies under the selective pressure of peramivir, the complete genomes of all the virus pools (passage 1 to 12) were analyzed by NGS. The coverage plots for the different gene segments of a representative sample was shown in Supplemental Fig. S1A. The average coverage across the whole genome for the sequenced samples was 268 ± 81. And the average coverage for HA and NA genes was 276 ± 89 and 227 ± 72, respectively (Supplemental Fig. S1B). The quasispecies polymorphism of Passage 1 virus analyzed by SNV calling was showed in Supplemental Table S3. Five gene segments of Passage 1 contained more than two SNV loci, with frequencies ranged from 8.06% to 42.86%. Strong selection is expected to reduce variation. However, the existence of peramivir seemed to have no effect on the genomewide nucleotide diversity of H7N9 virus (Fig. 2A). Then the frequencies of all SNVs across viral genome were tracked for 12 passages in both experimental and control groups (Fig. 2B and C). All the SNVs with mutation frequencies over 20% at passage 12 in both peramivir-treated group and control group were showed in Fig. 2D and E. The presence of peramivir caused an increase of SNVs that fixed at high frequencies especially over 80%, suggesting the variants rapidly evolved and became the dominant species in the virus quasispecies. Further analysis revealed these SNVs were mainly located at HA and NA genes (Fig. 2D). Remarkably, some mutations also arised in the absence of peramivir (Fig. 2E). The missense mutations included HA-707, HA-1484, PB2-1957, PB1-1201 and NP-469, with the corresponding amino acid substitutions of HA-S227Y, HA-T485I (H3 system numbering), PB2–S653T, PB1-A401T and NP-T157A, respectively.

3.3. Sequence analysis of viral NA gene

NA is the most important target for peramivir, thus the variation of NA under the selective pressure of peramivir was further analyzed. As shown in Table 1, by passage 12, two SNVs with high frequencies were detected in Passage 12-P2 virus, resulting in an amino acid substitution of I222T (95.89%) and a samesense mutation (76.36%), respectively. Two other substitutions, H274Y (86.90%) and V349I (10.79%) were detected in Passage 12-P3 virus. The I222T quasispecies emerged at passage 10, with a proportion of 9.68% which rose rapidly to 95.31% at passage 11 and reached 95.89% at passage 12. The H274Y quasispecies also emerged at passage 10, with a proportion of 39.82% which rose to 86.00% at passage 11 and reached 86.90% at passage 12. These data suggest I222T and H274Y might be beneficial mutations and positively selected in the environment of peramivir. The frequencies of other emerged SNVs (I444V, S267C, S171 N and V349I) were kept at low levels or below the minimum cutoff throughout the process of passage (Table 1). To evaluate whether the SNVs emerged in peramivir-treated group were specific to drug pressure, the variation of NA in the control group was also tracked for 12 passages. As shown in Supplemental Table S4, the I222T and H274Y quasispecies were not found in H7N9 virus in the control group. And by passage 12, no SNV with frequency above cutoff was detected.

To assess the fitness of drug-selected variants in the absence of drug, peramivir was either continued or withdrawn for 3 additional passages (Fig. 1B). As shown in Fig. 3A and B, the frequencies of I222T were maintained at > 99% since passage 13 regardless of the presence or absence of peramivir, and the frequencies of H274Y in the presence and absence of peramivir were maintained at > 99% and > 80%, respectively. However, the frequency of V349I increased from 10.79% to above 50% in the presence of peramivir, while decreased to below the minimum cutoff we set by passage 15 in the absence of drug (Fig. 3C). Then the SNVs in other 7 gene segments of peramivir-treated H7N9 virus at passage 12 (Fig. 2D) were further analyzed to identify mutaitons other than NA mutations which might neutralize the possible negative effects of I222T and H274Y mutations on virus fitness. The results showed that the NA-I222T-containing Passage 12-P2 virus pool had 3 amino acid mutations: HA-V186E (99.13%), HA-I268T (24.79%) and HA-M496T (55.04%, H3 system numbering), and the NA-H274Y-containing Passage 12-P3 virus pool had 6 mutations: HA-K101E

Table 3
IC_{50} values of NAIs in enzyme inhibition assay.

Virus	IC_{50} value (nM) [Mean (95% CI)] [Fold] [a]			
	Oseltamivir carboxylate	Peramivir	Zanamivir	Laninamivir
Passage 1	0.35 (0.32 - 0.39)	0.10 (0.10 - 0.11)	0.59 (0.54 - 0.64)	0.63 (0.59 - 0.66)
NA-I222T	3.02 (2.64 - 3.44) (8.63)	0.22 (0.20 - 0.24) (2.20)	1.71 (1.55 - 1.90) (2.90)	1.08 (1.01 - 1.15) (1.71)
NA-H274Y	46.06 (41.39 - 51.38) (131.60)	1.06 (0.95 - 1.18) (10.60)	1.50 (1.34 - 1.69) (2.54)	0.92 (0.86 - 0.98) (1.46)

[a] Fold change as compared with the IC_{50} value of Passage 1 virus. Fold increases of < 10, 10-100, and > 100 are interpreted as normal, reduced, and highly reduced inhibition using the criteria established by the WHO Inflenza Antiviral Working Group.

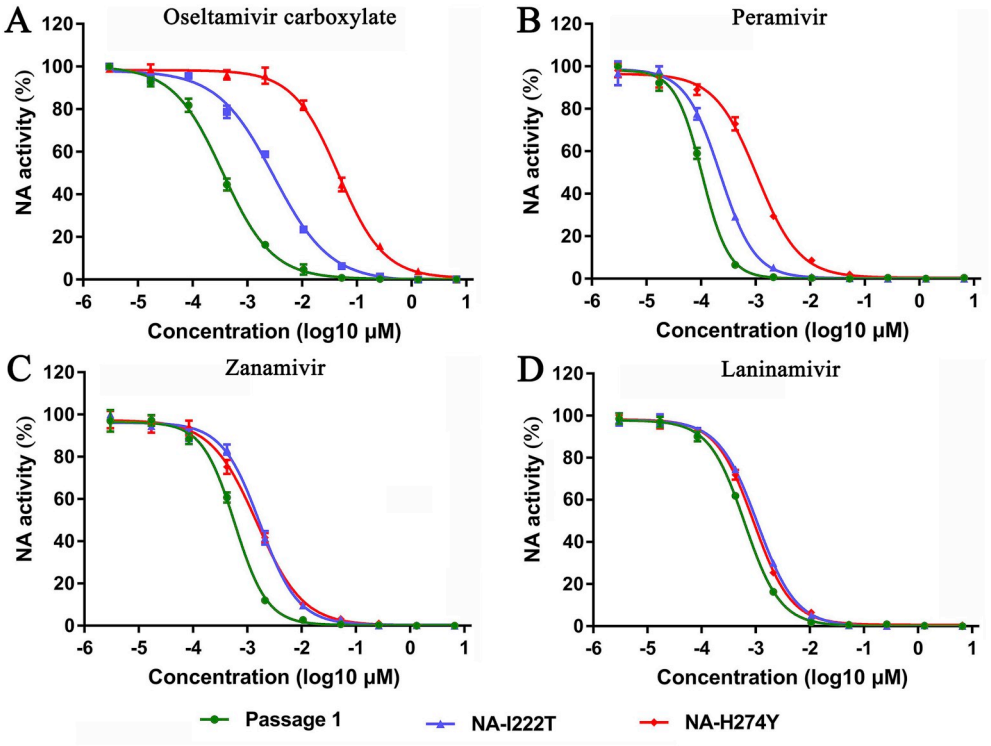

Fig. 4. Dose-response curves of the NA-I222T, NA-H274Y and Passage 1 viruses to four NAIs based on the results of enzyme-based NA inhibition assay. The NA activities of different viruses under increasing concentrations of oseltamivir (A), peramivir (B), zanamivir (C) and Laninamivir (D) were determined. Each data point represents the normalized neuraminidase activity (mean ± SD) from three replicated wells.

(98.26%), HA-A160T (100%), HA-E189A (100%), HA-N483Y (90.27%, H3 system numbering), NS-V157I (49.18%) and NS-G209S (48.94%).

3.4. Isolation and sequencing of NA-I222T and NA-H274Y variants

To investigate the effects of I222T and H274Y mutations on viral characteristics, plaque purification was performed to isolate individual clones from Passage 12-P2 and Passage 12-P3 viruses. Five clones of each virus were selected and the full genomes were analyzed by NGS. All the five clones of Passage 12-P2 were characterized by I222T, and four clones of Passage 12-P3 were characterized by H274Y. Based on the principle of minimal variation of full genome except NA, clone 3 of Passage 12-P2 (named NA-I222T) and clone 5 of Passage 12-P3 (named NA-H274Y) were chosen for further study. As shown in Table 2, sequencing results showed that the NA-I222T virus had one amino acid mutation (V186E) in HA as compared with Passage 1 virus, while the NA-H274Y virus had two mutations (K101E and N483Y). Besides, the A/T and E/A mixtures in HA of Passage 1 virus became homogeneous in both NA-I222T and NA-H274Y viruses. No additional mutations in the other six gene segments were observed in both the viruses. Both the NA-I222T and NA-H274Y viruses contained leucine (L) at HA-226 (H3 numbering), lysine (K) at PB2-627, aspartic acid (D) at PB2-701 and asparagines (N) at M2-31, the same as most of the previously reported H7N9 viruses.

3.5. In vitro susceptibility to NAIs in enzyme inhibition assay

The susceptibilities of plaque-purified viruses to four NAIs (oseltamivir, peramivir, zanamivir and Laninamivir) were determined using enzymatic methods. As shown in Table 3 and Fig. 4, the Passage 1 virus that was used as control was highly susceptible to all four NAIs, with low IC_{50} values. According to the criteria established by the WHO (WHO, 2012), the NA-H274Y virus exhibited highly reduced sensitivity to oseltamivir carboxylate and reduced sensitivity to peramivir, with IC_{50} values of 46.06 nM (131.6-fold) and 1.06 nM (10.6-fold), respectively. The NA-I222T virus showed no resistance to oseltamivir and peramivir in enzyme inhibition assay, with IC_{50} values of 3.02 nM (8.63-fold) and 0.22 nM (2.20-fold), respectively.

3.6. Susceptibility to NAIs and non-NAIs in virus yield reduction assay

Then we analyzed the sensitivities of NA-I222T and NA-H274Y viruses to oseltamivir carboxylate and peramivir in a cell-based virus yield reduction assay, and found that oseltamivir carboxylate exhibited poor inhibitory effects against both the NA-I222T (IC_{50}: 5.22 nM, 16.84-fold) and NA-H274Y (IC_{50}: 132.3 nM, 426.77-fold) viruses (Fig. 5 and Table 4). Peramivir exhibited poor inhibitory effects against NA-H274Y virus, with IC_{50} value of 4.09 nM (51.13-fold). Considering the decrease of susceptibility of mutant viruses to NAIs would directly affect the efficacy of clinical treatment, alternative therapeutic options to control

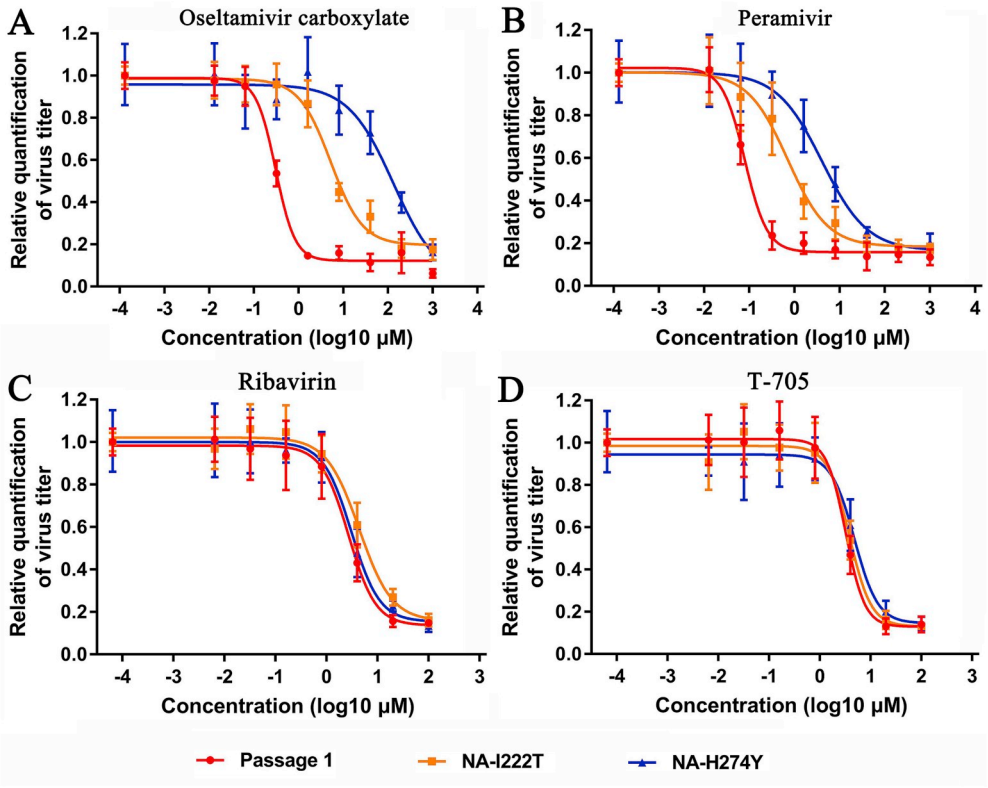

Fig. 5. Dose-response curves of the NA-I222T, NA-H274Y and Passage 1 viruses to NAIs and non-NAIs based on the results of cell-based virus yield reduction assay. MDCK cells were inoculated with different viruses and cultured in the absence or presence of various concentrations of oseltamivir (A), peramivir (B), ribavirin (C) and T705 (D) for 24h, after which cell-free supernatants were collected and the relative expression levels of H7 gene at different drug concentrations were quantified by real-time RT-PCR and normalized to control (no drug). Each data point represents the normalized relative expression level of H7 gene (mean ± SD) from three replicated wells.

Table 4
IC_{50} values of NAIs and non-NAIs in virus yield reduction assay.

Virus	IC_{50} value (μM) [Mean (95% CI)] [Fold][a]			
	Oseltamivir carboxylate	Peramivir	Ribavirin	T-705
Passage 1	0.31 (0.23 - 0.39)	0.08 (0.06 - 0.13)	2.71 (1.58 - 4.59)	3.24 (2.06 - 4.59)
NA-I222T	5.22 (3.23 - 9.47) (16.84)	0.71 (0.34 - 1.44) (8.88)	4.38 (2.67 - 8.72) (1.62)	3.83 (2.46 - 6.39) (1.18)
NA-H274Y	132.3 (N.A.) (426.77)	4.09 (1.84 - 9.37) (51.13)	3.07 (1.75 - 6.73) (1.13)	4.79 (2.88 - 10.56) (1.48)

N.A. not available.
[a] Fold change as compared with the IC_{50} value of Passage 1 virus.

these viruses is urgently needed. To this end, the inhibition of virus replication by two non-NAIs (T705 and ribavirin) at the cellular level was evaluated. The results showed that both the mutant viruses and Passage 1 virus exhibited comparable sensitivities to T705 and ribavirin (Fig. 5 and Table 4).

3.7. Virus replication kinetics in cell culture

To investigate the effects of I222T and H274Y mutations on viral proliferative property, the replication kinetics of both the viruses were assessed in MDCK cells. In order to further exclude the possible impact of HA mutations on viral fitness, we analyzed all the viral sequences from passage 1 to 12. We found that one parallel viral lineage from passage 4 treated with peramivir (Passage 4-P2) possessed the same genome sequences as NA-I222T virus except for the I222T mutation, and Passage 9-P3 virus possessed the same sequences as NA-H274Y virus except for the H274Y mutation in NA. Thus these two viruses were also used as control. As shown in Fig. 6, the Passage 1, Passage 4-P2, Passage 9-P3 and NA-I222T viruses showed efficient replication and produced comparable viral titers in MDCK cells, which peaked at 24–48 h post-infection. In contrast, the NA-H274Y virus exhibited delayed growth, with infectious titers lower than those of Passage 9-P3 viruses at 12, 24 and 36 h post-infection. However, the peak titer of NA-H274Y virus reached the same level as that of control after 48 h of infection.

3.8. Effect of the I222T and H274Y mutations on neuraminidase activity

To further evaluate whether the growth delay of NA-H274Y virus was related to the change of NA activity, kinetics assays were performed by using the fluorogenic substrate MUNANA. The NA-H274Y virus showed lower V_{max} and higher K_m (2.53-fold) values as compared with Passage 1 virus, suggesting the H274Y mutation led to decreased NA activity and reduced affinity for the substrate (Fig. 7 and Table 5). Therefore, impaired NA function caused by H274Y mutation might contribute to the growth delay of virus.

4. Discussion

With the use of NAIs, the evolution of H7N9 virus quasispecies and the mutation of NA affect not only viral drug resistance, but also enzymatic activity, fitness and pathogenicity, etc. (Marjuki et al., 2015; Zhang et al., 2014), which poses significant challenges for disease control. In this study, we systematically traced the evolutionary trajectories of H7N9 virus quasispecies under the selective pressure of peramivir by using NGS, and analyzed the effects of NA mutations caused by quasispecies evolution on the biological characteristics of H7N9 virus. We found that H7N9 virus quasispecies evolved under the

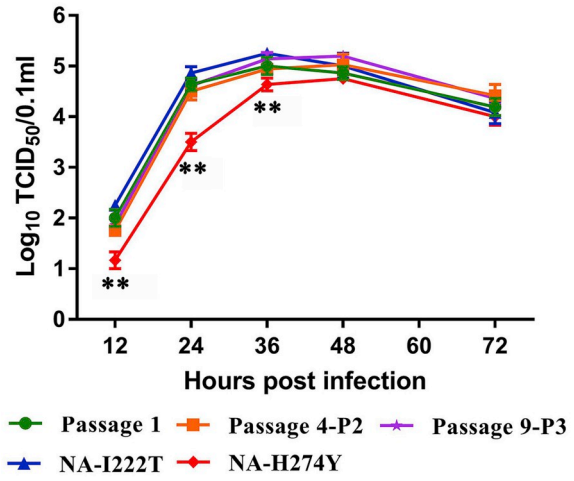

Fig. 6. Replication kinetics of H7N9 viruses in MDCK cells. MDCK cells were inoculated with the NA-I222T, NA-H274Y, Passage 4-P2, Passage 9-P3 and Passage 1 viruses at a MOI of 0.005 $TICD_{50}$ per cell. Cell-free supernatants were collected at indicated time points and titrated in MDCK cells by $TCID_{50}$ assay. Each data point represents the log_{10}-transformed $TCID_{50}$/0.1 ml (mean ± SD) from three replicated wells. $^{**}P < 0.01$, as compared with control (Passage 9-P3).

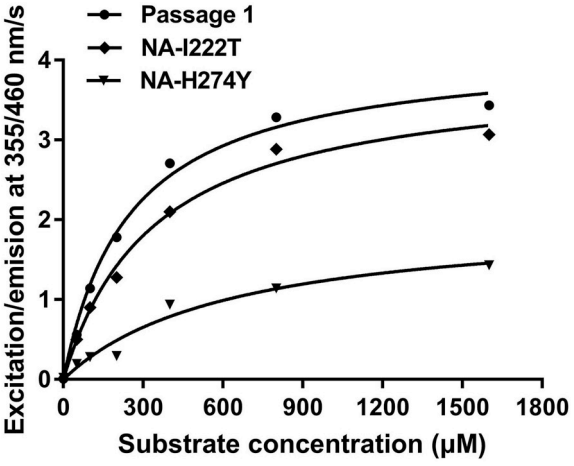

Fig. 7. NA enzymatic kinetics of the NA-I222T, NA-H274Y and Passage 1 viruses. The NA reaction rates at various substrate concentrations (0–1600 μM) were determined and expressed as the rates of fluorescence change (excitation/emission at 335/460 nm/s). The Michaelis constant (*Km*) and maximum velocity (*Vmax*) values of substrate conversion were determined by fitting enzyme kinetic data to the Michaelis-Menten equation.

selective pressure, leading to changes to the dominant populations of the virus. We also identified two important amino acid substitutions in NA (I222T and H274Y), which caused reduced susceptibilities to oseltamivir or both oseltamivir and peramivir as confirmed by enzyme- and cell-based assays. However, Non-NAI antivirals ribavirin and T-705 efficiently inhibited both the variants. Along with these results, we found the NA-H274Y variant exhibited decreased replicative fitness in MDCK cells at the early stage of infection and impaired NA function.

Quasispecies has been traditionally investigated by clone-based sequencing, which has low sensitivity and limited ability to detect low-abundance variants (Li et al., 2017). A highly accurate method is required to identify the extent of genetic variation in a virus quasispecies. NGS technology seems to fulfill this requirement. It can not only detect low-abundance variants, but also obtain the proportion of each variant, which can directly reflect the evolution process of virus quasispecies (Kuroda et al., 2010; Motro and Moran-Gilad, 2017; Yu et al., 2018). PCR amplification is commonly used in the library preparation for NGS to enrich the DNA fragments. However, it may introduce duplication, amplification bias and mutation, which are not conducive to quasispecies analysis (Huptas et al., 2016). To deliver the most accurate results, we adopted a PCR-free library preparation method which resulted in sufficient full-length coverage of influenza genome and depth of coverage for the study of quasispecies. Another hurdle has to be overcome is to distinguish between true mutations from errors introduced by the NGS chemistry. Among different high-throughput sequencing platforms, the Miseq has been reported to produce the highest quality reads, with a sequencing error rate of about 0.1% (Loman et al., 2012). After removing ambiguous nucleotides and trimming low quality bases, we excluded reads shorter than 50 nucleotides to avoid unspecific mapping. Van den Hoecke et al. showed that the detection limit for reliable recognition of variants in influenza genome required a frequency of 0.5% (higher than twice the sequencing error background) on miseq (Van den Hoecke et al., 2015). To minimize the false positive variant calls, we increased the cut-off value to 5%, above which the variant would be considered heterogeneous and biologically relevant.

Because of the resistance to amantadine conferred by S31 N substitution in the M2 protein, NAIs are the main drugs used for H7N9 treatment. It is disturbing that NAIs may not be always effective for treating H7N9 infections, even when the treatment is started early due to the emergence of resistant variants (Hu et al., 2013). In this study, we found the presence of peramivir caused an increase of SNVs that fixed at high frequencies, and these SNVs were mainly located at HA and NA genes. We also found some mutations arising in the absence of peramivir such as HA-S227Y, HA-T485I, PB2–S653T, PB1-A401T and NP-T157A, which might be attributed to the selective pressure of MDCK cells. Evidences show that amino acid changes in the HA at residue 227 (H3 system numbering) are critical for receptor binding activity of inflenza virus (Gambaryan et al., 2006). We speculate that the HA-S227Y mutation might alter the receptor specificity of H7N9 virus during adaptation to MDCK cells. Further analysis showed that two key amino acid substitutions (I222T and H274Y) occurred in the NA gene of H7N9 virus treated with peramivir. The I222T mutation has not previously been reported in 2013 H7N9 virus, while the H274Y mutation was found in a H7N9 patient by national influenza surveillance network in 2017 (Yang et al., 2017). Mutations introduced during viral replication are tolerated as they are neutral for virus fitness in the environment, rapidly lost as they reduce fitness, or expanded as they are advantageous (Lauring and Andino, 2010). The I222T and H274Y mutations in the NA of H7N9 virus might be advantageous for virus fitness in the environment of peramivir, because they rapidly expanded from passage 10 to 13. Although the withdrawn of peramivir had no significant effect on the variation frequencies of I222T and H274Y, we couldn't exclude the possibility that there were some permissive mutations which might neutralize the negative effects of I222T and H274Y mutations on virus fitness. Besides NA mutations, we found the Passage 12-P2 virus pool had 3 amino acid mutations (HA-V186E, HA-I268T and HA-M496T), and the Passage 12-P3 virus pool had 6 mutations (HA-K101E, HA-

Table 5
NA kinetics with the MUNANA substrate.

MUNANA	Passage 1	NA-I222T	NA-H274Y
K_m (μM) [mean (95% CI)]	250.0 (181.8 - 343.4)	343.2 (243.6 - 485.5)	633.4 (1.46 - 3.27)
V_{max} [mean (95% CI)]	4.15 (3.73 to 4.63)	3.87 (3.42 - 4.41)	2.04 (286.1 to 1618.0)

A160T, HA-E189A, HA-N483Y, NS-V157I and NS-G209S). Mutations at position 186 in the HA of A(H1N1)pdm09 and A/H3N2 viruses have been proved to be associated with virus replication in cell culture and eggs (Suphaphiphat et al., 2010; Gubareva et al., 1994). Whether the HA-V186E mutation identified in this study can increase the virus fitness of I222T variant, and whether the other mutations are associated with I222T and H274Y mutations still need to be further studied.

Although the I222T mutation has been reported in influenza A(H1N1)pdm09 virus and low-pathogenic avian influenza A(H7N9) virus in mallard model exposed to oseltamivir (Gillman et al., 2015; Huang et al., 2014), it is identified in 2013 H7N9 virus for the first time. Marjuki et al. demonstrated that I222K and I222R mutations in NA made H7N9 virus resistant to oseltamivir carboxylate with the IC_{50}-fold change ranged from 32 to 37 (Marjuki et al., 2015). Our results showed that the IC_{50} value of NA-I222T variant to oseltamivir carboxylate increased by 8.63-fold in enzyme-based assay, and 16.84-fold in cell-based assay. The H274Y mutation in NA of A(H1N1)pdm09 influenza viruses resulted in higher resistance to oseltamivir than to peramivir (Takashita et al., 2013). Consistent with this, we found the NA-H274Y variant of H7N9 virus also exhibited highly reduced sensitivity to oseltamivir and reduced sensitivity to peramivir, even though it was selected with peramivir. This might be because the mutation restricted the conformational change of E276 which was more important for the binding of oseltamivir to NA (Wang et al., 2002). . Notably, non-NAIs T705 and ribavirin retained their effectiveness against both the mutant viruses. Further animal studies should be performed to confirm whether these non-NAIs could still be effective against the NA-N222T and NA-H274Y variants even when administered post infection, because the antiviral therapy for H7N9 patients is often delayed.

It has been proved that the mutation of NA not only affects viral sensitivity to NAIs, but also other biological characteristics of influenza virus such as enzymatic activity, fitness and pathogenicity (Marjuki et al., 2015; Wu et al., 2013; Zhang et al., 2014). The R294K substitution in NA of A/Shanghai/1/2013(H7N9) virus resulted in multi-drug resistance along with reduced NA activity and lower viral fitness (Wu et al., 2013). Consistently, the NA-R292K variant isolated from an oseltamivir-treated H7N9 patient showed reduced replicative fitness in both MDCK-SIAT1 cells and ferrets, while the NA-I222K and NA-I222R variants did not (Marjuki et al., 2015). By evaluation of viral replication kinetics in MDCK cells, we found that viral growth was slightly impaired for the NA-H274Y variant at the early stage of infection, while there was almost no difference in the growth for NA-I222T variant. These data are similar to that found in influenza A(H1N1)pdm09 virus (Huang et al., 2014). The kinetics assay of NA revealed the impaired NA function caused by H274Y mutation might contribute to the growth delay of the virus.

In conclusion, we report here the evolution of H7N9 virus quasispecies under the selective pressure of peramivir *in vitro*, and the effects of key amino acid substitutions in NA on the biological characteristics of the virus. The potential emergence and possible community transmission of the NA-I222T and NA-H274Y variants, as well as the quasispecies evolution of H7N9 virus under various selective pressures should be closely monitored, which may provide guidance for the prevention and clinical medication of H7N9 avian influenza.

Declarations of interest

None.

Acknowledgments

This work was supported in part by the National Natural Science Foundation of China (81601732, 81501785, 81871666), the Natural Science Foundation of Jiangsu Province (BK20161583, BK20141030), the National Major Science & Technology Projects for Infectious Disease Control and Prevention (2017ZX10103008), the Jiangsu Provincial Key Medical Discipline of Epidemiology (ZDXKA2016008), the Jiangsu Provincial Medical Youth Talent (QNRC2016537), the “333” Project (BRA2017552) and “Six One” Project (LGY2017084) of Jiangsu Province.

Appendix A. Supplementary data

Supplementary data to this article can be found online at https://doi.org/10.1016/j.virol.2019.08.004.

References

CDC, 2017. Summary of influenza risk assessment Tool (IRAT) results. Available. https://www.cdc.gov/flu/pandemic-resources/monitoring/irat-virus-summaries.htm, Accessed date: 18 July 2019.

Domingo, E., Sheldon, J., Perales, C., 2012. Viral quasispecies evolution. Microbiol. Mol. Biol. Rev. 76, 159–216.

Drake, J.W., Holland, J.J., 1999. Mutation rates among RNA viruses. Proc. Natl. Acad. Sci. U.S.A. 96, 13910–13913.

Gambaryan, A., Tuzikov, A., Pazynina, G., Bovin, N., Balish, A., Klimov, A., 2006. Evolution of the receptor binding phenotype of influenza A (H5) viruses. Virology 344, 432–438.

Gao, R., Cao, B., Hu, Y., Feng, Z., Wang, D., Hu, W., Chen, J., Jie, Z., Qiu, H., Xu, K., Xu, X., Lu, H., Zhu, W., Gao, Z., Xiang, N., Shen, Y., He, Z., Gu, Y., Zhang, Z., Yang, Y., Zhao, X., Zhou, L., Li, X., Zou, S., Zhang, Y., Li, X., Yang, L., Guo, J., Dong, J., Li, Q., Dong, L., Zhu, Y., Bai, T., Wang, S., Hao, P., Yang, W., Zhang, Y., Han, J., Yu, H., Li, D., Gao, G.F., Wu, G., Wang, Y., Yuan, Z., Shu, Y., 2013. Human infection with a novel avian-origin influenza A (H7N9) virus. N. Engl. J. Med. 368, 1888–1897.

Gillman, A., Nykvist, M., Muradrasoli, S., Soderstrom, H., Wille, M., Daggfeldt, A., Brojer, C., Waldenstrom, J., Olsen, B., Jarhult, J.D., 2015. Influenza A(H7N9) virus acquires resistance-related neuraminidase I222T substitution when infected mallards are exposed to low levels of oseltamivir in water. Antimicrob. Agents Chemother. 59, 5196–5202.

Gubareva, L.V., Wood, J.M., Meyer, W.J., Katz, J.M., Robertson, J.S., Major, D., Webster, R.G., 1994. Codominant mixtures of viruses in reference strains of influenza virus due to host cell variation. Virology 199, 89–97.

Hoffmann, E., Stech, J., Guan, Y., Webster, R.G., Perez, D.R., 2001. Universal primer set for the full-length amplification of all influenza A viruses. Arch. Virol. 146, 2275–2289.

Hu, Y., Lu, S., Song, Z., Wang, W., Hao, P., Li, J., Zhang, X., Yen, H.L., Shi, B., Li, T., Guan, W., Xu, L., Liu, Y., Wang, S., Zhang, X., Tian, D., Zhu, Z., He, J., Huang, K., Chen, H., Zheng, L., Li, X., Ping, J., Kang, B., Xi, X., Zha, L., Li, Y., Zhang, Z., Peiris, M., Yuan, Z., 2013. Association between adverse clinical outcome in human disease caused by novel influenza A H7N9 virus and sustained viral shedding and emergence of antiviral resistance. Lancet 381, 2273–2279.

Huang, L., Cao, Y., Zhou, J., Qin, K., Zhu, W., Zhu, Y., Yang, L., Wang, D., Wei, H., Shu, Y., 2014. A conformational restriction in the influenza A virus neuraminidase binding site by R152 results in a combinational effect of I222T and H274Y on oseltamivir resistance. Antimicrob. Agents Chemother. 58, 1639–1645.

Huptas, C., Scherer, S., Wenning, M., 2016. Optimized Illumina PCR-free library preparation for bacterial whole genome sequencing and analysis of factors influencing de novo assembly. BMC Res. Notes 9, 269.

Iuliano, A.D., Jang, Y., Jones, J., Davis, C.T., Wentworth, D.E., Uyeki, T.M., Roguski, K., Thompson, M.G., Gubareva, L., Fry, A.M., Burns, E., Trock, S., Zhou, S., Katz, J.M., Jernigan, D.B., 2017. Increase in human infections with avian influenza A(H7N9) virus during the fifth epidemic - China, october 2016-february 2017. MMWR Morb. Mortal. Wkly. Rep. 66, 254–255.

Kuroda, M., Katano, H., Nakajima, N., Tobiume, M., Ainai, A., Sekizuka, T., Hasegawa, H., Tashiro, M., Sasaki, Y., Arakawa, Y., Hata, S., Watanabe, M., Sata, T., 2010. Characterization of quasispecies of pandemic 2009 influenza A virus (A/H1N1/2009) by de novo sequencing using a next-generation DNA sequencer. PLoS One 5, e10256.

Lauring, A.S., Andino, R., 2010. Quasispecies theory and the behavior of RNA viruses. PLoS Pathog. 6, e1001005.

Loman, N.J., Misra, R.V., Dallman, T.J., Constantinidou, C., Gharbia, S.E., Wain, J., Pallen, M.J., 2012. Performance comparison of benchtop high-throughput sequencing platforms. Nat. Biotechnol. 30, 434–439.

Li, J., Wang, M., Yu, D., Han, Y., Yang, Z., Wang, L., Zhang, X., Liu, F., 2017. A comparative study on the characterization of hepatitis B virus quasispecies by clone-based sequencing and third-generation sequencing. Emerg. Microb. Infect. 6, e100.

Li, Y., Wu, T., Qi, X., Ge, Y., Guo, X., Wu, B., Yu, H., Zhu, Y., Shi, Z., Wang, H., Cui, L., Zhou, M., 2013. Simultaneous detection of hemagglutinin and neuraminidase genes of novel influenza A (H7N9) by duplex real-time reverse transcription polymerase chain reaction. J. Virol. Methods 194, 194–196.

Lu, J., Raghwani, J., Pryce, R., Bowden, T.A., Theze, J., Huang, S., Song, Y., Zou, L., Liang, L., Bai, R., Jing, Y., Zhou, P., Kang, M., Yi, L., Wu, J., Pybus, O.G., Ke, C., 2018. Molecular evolution, diversity, and adaptation of influenza A(H7N9) viruses in China. Emerg. Infect. Dis. 24, 1795–1805.

Marjuki, H., Mishin, V.P., Chesnokov, A.P., Jones, J., De La Cruz, J.A., Sleeman, K., Tamura, D., Nguyen, H.T., Wu, H.S., Chang, F.Y., Liu, M.T., Fry, A.M., Cox, N.J., Villanueva, J.M., Davis, C.T., Gubareva, L.V., 2015. Characterization of drug-resistant influenza A(H7N9) variants isolated from an oseltamivir-treated patient in Taiwan. J. Infect. Dis. 211, 249–257.

Motro, Y., Moran-Gilad, J., 2017. Next-generation sequencing applications in clinical bacteriology. Biomol Detect Quantif 14, 1–6.
Suphaphiphat, P., Franti, M., Hekele, A., Lilja, A., Spencer, T., Settembre, E., Palmer, G., Crotta, S., Tuccino, A.B., Keiner, B., Trusheim, H., Balabanis, K., Sackal, M., Rothfeder, M., Mandl, C.W., Dormitzer, P.R., Mason, P.W., 2010. Mutations at positions 186 and 194 in the HA gene of the 2009 H1N1 pandemic influenza virus improve replication in cell culture and eggs. Virol. J. 7, 157.
Takashita, E., Fujisaki, S., Kishida, N., Xu, H., Imai, M., Tashiro, M., Odagiri, T., 2013. Influenza Virus Surveillance Group of, J.Characterization of neuraminidase inhibitor-resistant influenza A(H1N1)pdm09 viruses isolated in four seasons during pandemic and post-pandemic periods in Japan. Influenza Other Respir Viruses 7, 1390–1399.
Taubenberger, J.K., Kash, J.C., 2010. Influenza virus evolution, host adaptation, and pandemic formation. Cell Host Microbe 7, 440–451.
Van den Hoecke, S., Verhelst, J., Vuylsteke, M., Saelens, X., 2015. Analysis of the genetic diversity of influenza A viruses using next-generation DNA sequencing. BMC Genomics 16, 79.
Wang, D., Yang, L., Zhu, W., Zhang, Y., Zou, S., Bo, H., Gao, R., Dong, J., Huang, W., Guo, J., Li, Z., Zhao, X., Li, X., Xin, L., Zhou, J., Chen, T., Dong, L., Wei, H., Li, X., Liu, L., Tang, J., Lan, Y., Yang, J., Shu, Y., 2016. Two outbreak sources of influenza a (H7N9) viruses have been established in China. J. Virol. 90, 5561–5573.
Wang, M.Z., Tai, C.Y., Mendel, D.B., 2002. Mechanism by which mutations at his274 alter sensitivity of influenza a virus n1 neuraminidase to oseltamivir carboxylate and zanamivir. Antimicrob. Agents Chemother. 46, 3809–3816.
WHO, 2018. Human infection with avian influenza A(H7N9) virus - China: update, 5 September 2018. Available. http://www.who.int/csr/don/05-september-2018-ah7n9-china/en/, Accessed date: 21 March 2019.
WHO, 2013. Serological detection of avian influenza A(H7N9) infections by microneutralization assay, 23 May 2013. Available. http://www.who.int/influenza/gisrs_laboratory/cnic_serological_diagnosis_microneutralization_a_h7n9.pdf, Accessed date: 21 March 2019.
WHO, 2012. Meetings of the WHO working group on surveillance of inflenza antiviral susceptibility-Geneva, November 2011 and June 2012. Wkly. Epidemiol. Rec. 87, 369–374.
Wu, Y., Bi, Y., Vavricka, C.J., Sun, X., Zhang, Y., Gao, F., Zhao, M., Xiao, H., Qin, C., He, J., Liu, W., Yan, J., Qi, J., Gao, G.F., 2013. Characterization of two distinct neuraminidases from avian-origin human-infecting H7N9 influenza viruses. Cell Res. 23, 1347–1355.
Xiao, Y.L., Ren, L., Zhang, X., Qi, L., Kash, J.C., Xiao, Y., Wu, F., Wang, J., Taubenberger, J.K., 2018. Deep sequencing of H7N9 influenza a viruses from 16 infected patients from 2013 to 2015 in shanghai reveals genetic diversity and antigenic drift. mSphere 3, e00462 00418.
Yang, L., Zhu, W., Li, X., Chen, M., Wu, J., Yu, P., Qi, S., Huang, Y., Shi, W., Dong, J., Zhao, X., Huang, W., Li, Z., Zeng, X., Bo, H., Chen, T., Chen, W., Liu, J., Zhang, Y., Liang, Z., Shi, W., Shu, Y., Wang, D., 2017. Genesis and spread of newly emerged highly pathogenic H7N9 avian viruses in mainland China. J. Virol. 91, e01277 01217.
Yen, H.L., McKimm-Breschkin, J.L., Choy, K.T., Wong, D.D., Cheung, P.P., Zhou, J., Ng, I.H., Zhu, H., Webby, R.J., Guan, Y., Webster, R.G., Peiris, J.S., 2013. Resistance to neuraminidase inhibitors conferred by an R292K mutation in a human influenza virus H7N9 isolate can be masked by a mixed R/K viral population. mBio 4, e00396 00313.
Yu, D., Xiang, G., Zhu, W., Lei, X., Li, B., Meng, Y., Yang, L., Jiao, H., Li, X., Huang, W., Wei, H., Zhang, Y., Hai, Y., Zhang, H., Yue, H., Zou, S., Zhao, X., Li, C., Ao, D., Zhang, Y., Tan, M., Liu, J., Zhang, X., Gao, G.F., Meng, L., Wang, D., 2019. The re-emergence of highly pathogenic avian influenza H7N9 viruses in humans in mainland China, 2019. Euro Surveill. 24.
Yu, F., Wen, Y., Wang, J., Gong, Y., Feng, K., Ye, R., Jiang, Y., Zhao, Q., Pan, P., Wu, H., Duan, S., Su, B., Qiu, M., 2018. The transmission and evolution of HIV-1 quasispecies within one couple: a follow-up study based on next-generation sequencing. Sci. Rep. 8, 1404.
Zhang, X., Song, Z., He, J., Yen, H.L., Li, J., Zhu, Z., Tian, D., Wang, W., Xu, L., Guan, W., Liu, Y., Wang, S., Shi, B., Zhang, W., Qin, B., Cai, J., Wan, Y., Xu, C., Ren, X., Chen, H., Liu, L., Yang, Y., Zhou, X., Zhou, W., Xu, J., Zhang, X., Peiris, M., Hu, Y., Yuan, Z., 2014. Drug susceptibility profile and pathogenicity of H7N9 influenza virus (Anhui1 lineage) with R292K substitution. Emerg. Microb. Infect. 3, e78.
Zhu, W., Zhou, J., Li, Z., Yang, L., Li, X., Huang, W., Zou, S., Chen, W., Wei, H., Tang, J., Liu, L., Dong, J., Wang, D., Shu, Y., 2017. Biological characterisation of the emerged highly pathogenic avian influenza (HPAI) A(H7N9) viruses in humans, in mainland China, 2016 to 2017. Euro Surveill. 22, 30533.